Article

Efficient Removal of Eriochrome Black T Dye Using Activated Carbon of Waste Hemp (*Cannabis sativa* L.) Grown in Northern Morocco Enhanced by New Mathematical Models

Fouad El Mansouri [1,*], Guillermo Pelaz [2], Antonio Morán [2], Joaquim C. G. Esteves Da Silva [3], Francesco Cacciola [4,*], Hammadi El Farissi [5], Hatim Tayeq [6], Mohammed Hassani Zerrouk [7] and Jamal Brigui [1]

[1] Research Team: Materials, Environment and Sustainable Development (MEDD), Faculty of Sciences and Techniques of Tangier, BP 416, Tangier 90000, Morocco
[2] Chemical and Environmental Bioprocess Engineering Group, Natural Resources Institute, University of León, 24071 León, Spain
[3] Centro de Investigação Em Química (CIQUP), Instituto De Ciências Moleculares (IMS), Departamento De Geociências, Ambiente e Ordenamento Do Território, Faculdade De Ciências, Universidade Do Porto, Rua Do Campo Alegre S/N, 4169-007 Porto, Portugal
[4] Department of Biomedical, Dental, Morphological and Functional Imaging Sciences, University of Messina, 98125 Messina, Italy
[5] Laboratory of Environment and Applied Chemistry of the Natural Resources and Processes, Department of Chemistry, Faculty of Sciences, Mohamed First University, BP 524, Oujda 60000, Morocco
[6] MAE2D Laboratory, Polydisciplinary Faculty of Larache, Abdelmalek Essaadi University, Tetouan 93020, Morocco
[7] Environmental Technologies, Biotechnology and Valorisation of Bio-Resources Team, TEBVB, FSTH, Abdelmalek Essaadi University, Tetouan 93020, Morocco
* Correspondence: fouad.elmansouri@etu.uae.ac.ma (F.E.M.); cacciolaf@unime.it (F.C.);
  Tel.: +212-662-102-847 (F.E.M.); +39-090-676-6570 (F.C.)

Highlights:

- The use of inexpensive, easily obtained, and ecological adsorbents.
- New bio-adsorbents were made for Colorant adsorption from an aqueous solution.
- EBT dye adsorption capacities ranged from 1.8 to 2.8 mg.g^{-1}.
- Adsorptions of EBT dye by the activated carbon of cannabis.
- This study provides cost-effective and sustainable production of activated carbon.
- Application of mathematical modeling to develop new relevant mathematical models based on experimental results.

Abstract: In the present work, the adsorption behavior of Eriochrome Black T (EBT) on waste hemp activated carbon (WHAC) was examined. The surface of the WHAC was modified by H_3PO_4 acid treatment. The surface and structural characterization of the adsorbents was carried out using Fourier transform infrared spectroscopy (FTIR), and scanning electron microscopy (SEM) analysis. The effect of influential adsorption parameters (pH, contact time, dosage, and initial concentration) on the adsorption of EBT onto WHAC was examined in batch experiments; some adsorption parameters such as pH, concentration and dose were improved by new mathematical models. The adsorption behavior of EBT on the surfaces of WHAC was evaluated by applying different isotherm models (Langmuir, Freundlich, Temkin and Dubinin–Radushkevich) to equilibrium data. The adsorption kinetics was studied by using pseudo-first-order, pseudo-second-order, Elovich and intraparticle models on the model. Adsorption followed the pseudo-second-order rate kinetics. The maximum removal of EBT was found to be 44–62.08% by WHAC at pH = 7, adsorbent dose of 10–70 mg, contact time of 3 h and initial dye concentration of 10 mg.L^{-1}. The maximum adsorption capacities were 14.025 mg.g^{-1} obtained by calculating according to the Langmuir model, while the maximum removal efficiency was obtained at 70 mg equal to 62.08% for the WHAC. The adsorption process is physical in the monolayer and multilayer.

1. Introduction

Hemp or (*Cannabis sativa* L.), is an annual herbaceous plant, belonging to the family of Cannabaceae, and originating in Central Asia. Regardless of its origin, hemp is commonly grown and cultivated not only in Asian countries [1] but in Africa, Europe, Canada, and the United States, and is one of the oldest cultivated plants known to humans. Since 5000–4000 BC, [2], it has been used as a food and fiber source, as well as playing an important role in medical use. It contains several chemically bioactive compounds, such as cannabinoids, terpenoids, flavonoids, and alkaloids [3]. It contains more than 100 active chemical compounds well-known as 'cannabinoids' [4].

Waste is a major worldwide problem and produces severe ecological and socio-economic troubles. The exploitation of waste has become of vast scientific and industrial importance in order to reduce ecological harm, attain sustainability and progress, apropos a circular economy. Energy, fuels, and other value-added products can be recuperated from waste [5]. Moreover, owing to the fast growth in the quantity and nature of agricultural waste biomass, which comes from the growth of population and rigorous agricultural behaviors, these wastes are deemed as a consequential cause of pollution with an annual growth frequency of 5–10%. People produce about 150 billion metric tons of agricultural waste [6].

As a biological and ecological alternative, the application of agro-waste as precursors of materials with high adsorptive abilities is being explored [7]. Bio-adsorbents (bioproducts) are natural elements suitable for water treatment in view of the many benefits and remarkable characteristics of these assets. They are ample, inexhaustible, decomposable, and economic [8], moreover, they have macromolecular chains with various extremely reactive chemical functions [9]. In addition, adsorption is designed within the effective methods for the elimination of water contaminants because of its facility of function and the aptitude to eliminate various kinds of contaminants, providing larger application in water quality management [10].

Amid the diversity of adsorbents, activated carbon has been demonstrated to remain efficient in the elimination of contaminants from water and even in a gaseous atmosphere [11] Activated carbon, a commonly used adsorbent in industrial procedures, is constituted of a pored, consistent organization with a great surface area and displays radiation stability [12]. On the other hand, its application is restricted because it is expensive and very difficult to be regenerated [13,14]. Therefore, an investigation of the fabrication of activated carbon from inexhaustible, inexpensive native farming waste has won interest due to its reduced cost and extremely plentiful qualities [15,16]; in this context, certain of the farming wastes that have been investigated as an alternative source of activated carbon are barley seeds [17], orange peel [18], cassava peel [19], eucalyptus bark [20], coconut shells [21], hazel nuts [22], and tobacco steam [23].

Eriochrome Black T (EBT) is one of the colorants that are employed in water hardness resolution, in the production of paper and textiles, and also in the biomedical research field [24]. It was identified as a water pollutant which causes substantial damage to the environment. EBT is an organic azo colorant that is tolerant to natural treatment as most azo colorants are, due to their aromatic rings and sulfonate groups. Even at reduced amounts, it is not easily decayed by chemical or bacterial deterioration [25].

The overall objective of this study is to report the synthesis and characterization of hemp waste (*Cannabis sativa* L.) and its activated carbon. The as-synthesized materials were used as adsorbents for the removal of Eriochrome Black T dye in an aqueous solution. The effects of various experimental parameters on the adsorption of the dye were examined. The adsorption parameters (pH, concentration, and dose) were improved by new mathematical models obtained with a polynomial interpolation.

2. Materials and Methods

In the current study, activated carbon was geared up from residues of *Cannabis sativa* L. with the saturation of a chemical activating agent at reduced temperatures. We note there are only a few limited studies on the elimination of Eriochrome Black T dye using *Cannabis sativa* L. activated carbon as an adsorbent. All chemicals employed in this work were of analytical grade and were used without additional purification.

2.1. Preparation of Waste Hemp Activated Carbon (WHAC)

The method of preparation applied for the WHAC has two steps: carbonization and activation, as already described in our previous works [26,27]. After impregnation, to remove any excess of phosphoric acid, the solid was filtered under a vacuum. Then afterwards the waste hemp powder was pyrolyzed at 600 °C for 90 min in a muffle furnace (PR Series Hobersal). Furthermore, the carbon was completely washed with ultra-pure water to remove the remaining phosphoric acid until reaching a pH of (6.5). Lastly, the solids were dried in the oven at 105 °C for 24 h

2.2. Characterization of the Activated Carbon

In order to approximate the temperature of distribution at which waste hemp responds under a latent climate, a thermogravimetric analysis (TGA) was applied. Thermal analyses were conducted with STD 2960 TA and SDT Q600 instruments under a nitrogen flow of 100 mL/min. A temperature ramp of 10 °C/min from room temperature to 800 °C was employed during the analyses.

FTIR spectroscopy was used to examine the surface functionalities. A Thermo IS5 Nicolet (USA) spectrophotometer was used to obtain FTIR spectra, acquired from 400 to 4000 cm^{-1} at room temperature (16 scans and spectral resolution of 4 cm^{-1}); the peak positions were revealed using Origin software (Version 2021). Origin Lab Corporation, Northampton, MA, USA.

2.3. Functional Group Analysis by FTIR

To characterize the different functional groups at the surface of the precursor and the prepared activated carbon, FTIR spectra of the various materials (EBTA, WHAC, WHNAC, WH, WHAFC) were recorded between 4000 cm^{-1} to 400 cm^{-1}. Figure 1 depicts the obtained spectrum. From this figure, the precursor presents vibration bands around 607.46, 691.12, 862.02, 953.62; 1028.83, 1086.69, 1230.20, 1306.5, 1394.28, 1616.05, 1741.4, 2851.52, 2920.66 and 3291.89 cm^{-1}. The infrared spectrum of the mixture remaining after the adsorption of the EBTA colorant displays a total absence of the waves linked to the dye, obtaining two bungs which correspond to the water molecule, one bung at 3291.89 cm^{-1} and the other at 1616.05 cm^{-1}. On one hand, the WHAC carbonization and the WHAFC activation of the carbon present cyclic carbon compounds, and functional groups have disappeared such as alcohols, ketones, and aldehydes. On the other hand, the biomass is rich in witness groups and also present in addition to the OH groups linked to 3300 cm^{-1}. The table indicates the different leaves that contain cannabis. The other bonds are grouped in Table 1, where:
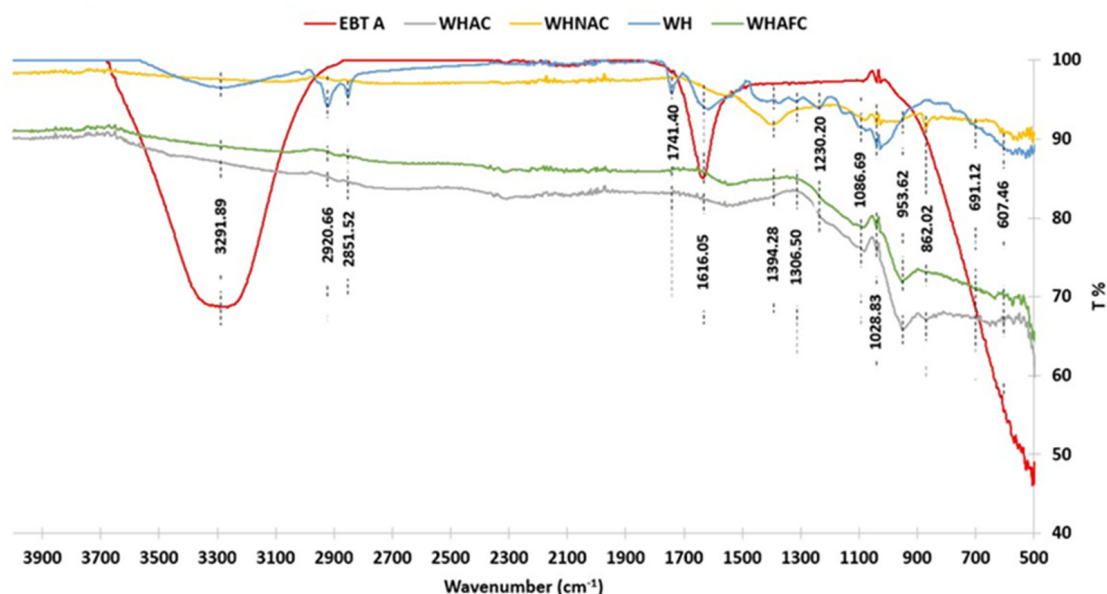
EBT-A: Eriochrome Black T after adsorption and filtration.
WHAC: waste hemp activated carbon.
WHNAC: waste hemp non-activated carbon.
WH: waste hemp (*Cannabis sativa* L.).
WHAFC: waste hemp activated carbon after adsorption.

Figure 1. FTIR (Fourier transform infrared spectroscopy) spectra.

Table 1. FTIR analysis of WHAC.

Bond Type	Functional Group	Wave Numbers Range (cm^{-1})	
		σ_{th}	σ_{exp}
C-H	Alkane	2850–2925	2920.66
			2851.52
C=O	Aliphatic Ketone	1710–1735	1741.40
C-H	Aldehyde	1370–1390	1394.28
C-OH	Third Alcohol	1110–1250	1230.20
			1146.47
C-H	Cycloalkane	1012–1031	1028.83
=C-H (E)	Alkene	950–1010	953.62
Ar-C	Aromatic	850–890	862.02
=C-H (Z)	Alkene	650–750	691.12

2.4. SEM/EDX

SEM micrographs and elemental analysis spectra of various prepared materials shown in Figure 2 show that all the materials have cracks and pores on their surfaces. This may be due to the escape of gases released during the carbonization process [28,29]. As the rate of impregnation increases, the development of cracks and pores becomes more pronounced. The prepared materials consist mainly of carbon (47.85 to 54.70%), oxygen (28.72 to 36.57%), phosphorus (0.35 to 12.14%), calcium (0.88 to 6.41%), and silicon (0.27 to 1.09%). Other elements such as magnesium, aluminum, sulfur, potassium, and sodium are present in the form of traces, in Figure 3. The high carbon content coupled with the porous structure of all the materials prepared are important criteria for an adsorbent suitable for the elimination of colorants and heavy metals in an aqueous media [30].
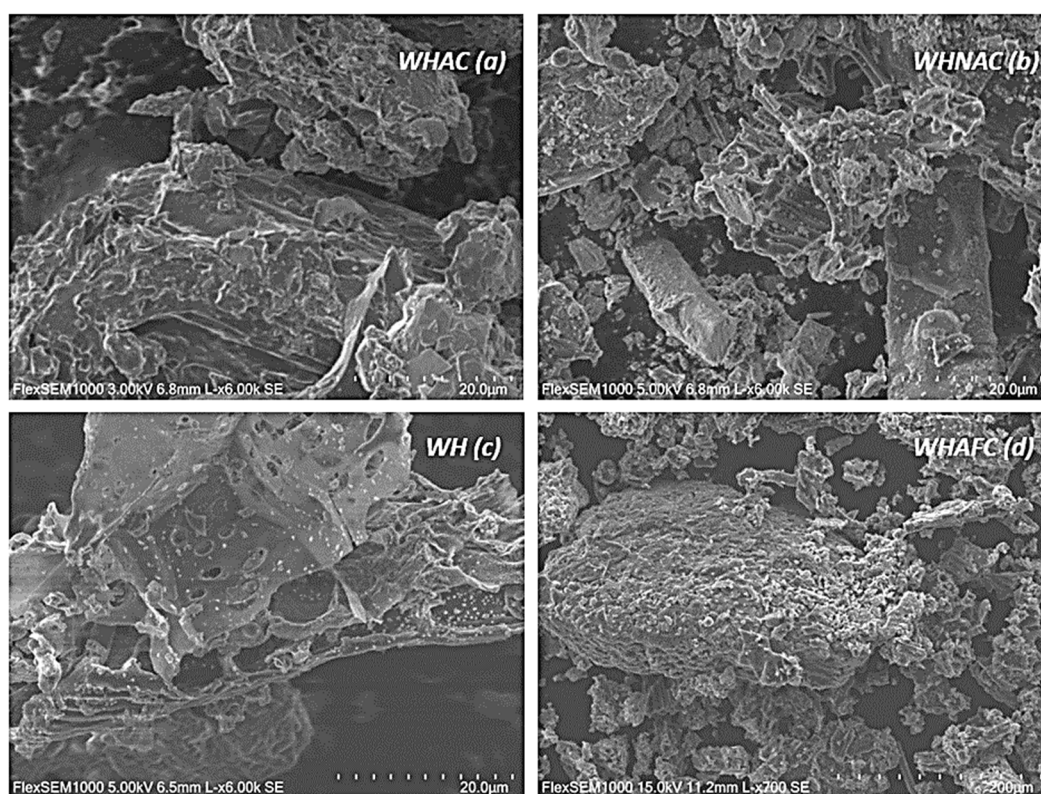
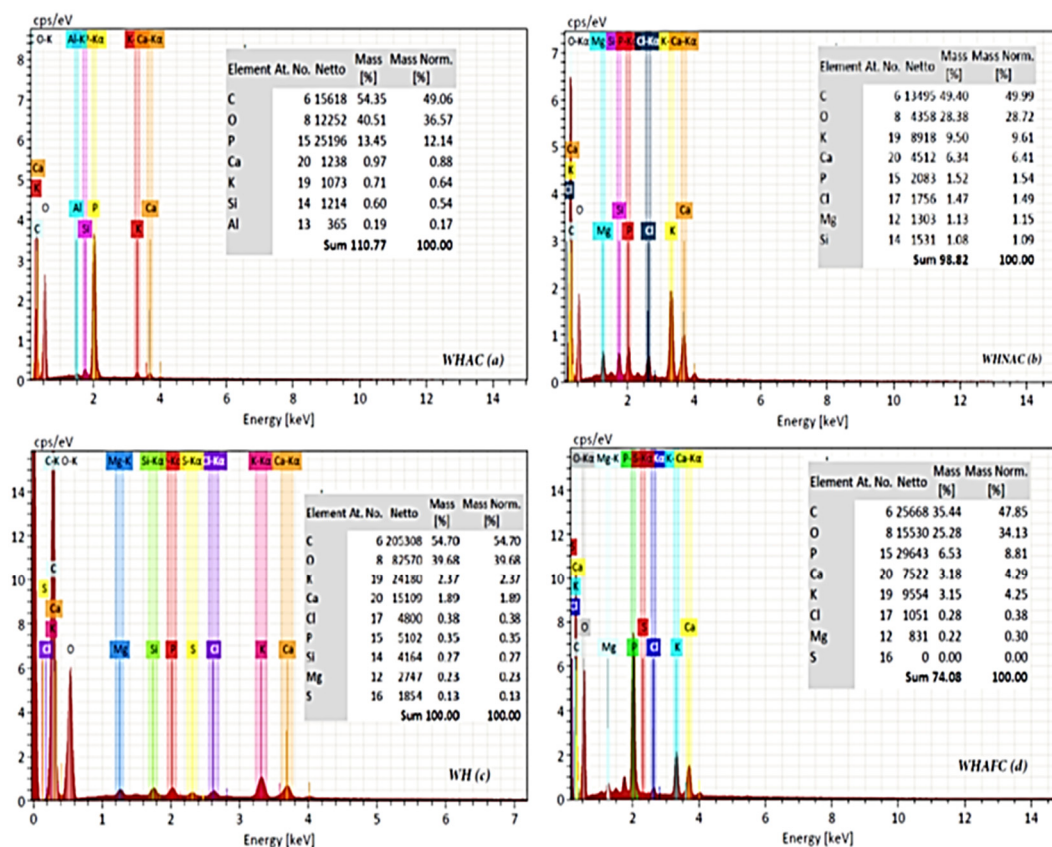**Figure 2.** SEM (scanning electron microscopy) micrographs.

Figure 3. EDXA (energy dispersive X-ray analysis) diffractograms.

2.5. TGA/DTA Analysis

The waste hemp (*Cannabis sativa* L.) thermal performance was examined employing thermogravimetric analysis (TGA) and differential scanning calorimetry (DSC). Figure 4 depicts the TGA/DSC curve of WH for the heating rate of 50 °C/min. As a result, the thermal decomposition of WH was detected at three phases. The first phase occurs from room temperature to about 125 °C with a corresponding weight loss of 9.9%. The endothermic process that takes place at 81 °C could be assigned to the vaporization of water. The low value of weight loss at this stage is a result of the low moisture content of WH. In the second phase, which extends up to about 320 °C, the weight loss has considerably increased to a value of 56.33%. At this stage, the broad and intense exothermic peak detected at 304 °C can be attributed to the decomposition of celluloses, hemicelluloses, and part of lignin. According to Haykiri et al. [31], hemicellulose and part of lignin decomposes in the range 265–310 °C. During the third phase, there is a narrow peak centered at 405 °C which relates to the degradation of residual lignin. This phase corresponds to the combustion of released gases during the decomposition of lignin. In this phase, the mass loss was lower than in the previous phase corresponding to 31.07%. The shoulder at 373 °C corresponds to the transition from the combustion of celluloses to lignin [32]. Above 505 °C the weight loss becomes constant. This shows that all the lignocellulosic content has been decomposed. Therefore, T = 505 °C appears as a minimum temperature to produce WH-based activated carbon.
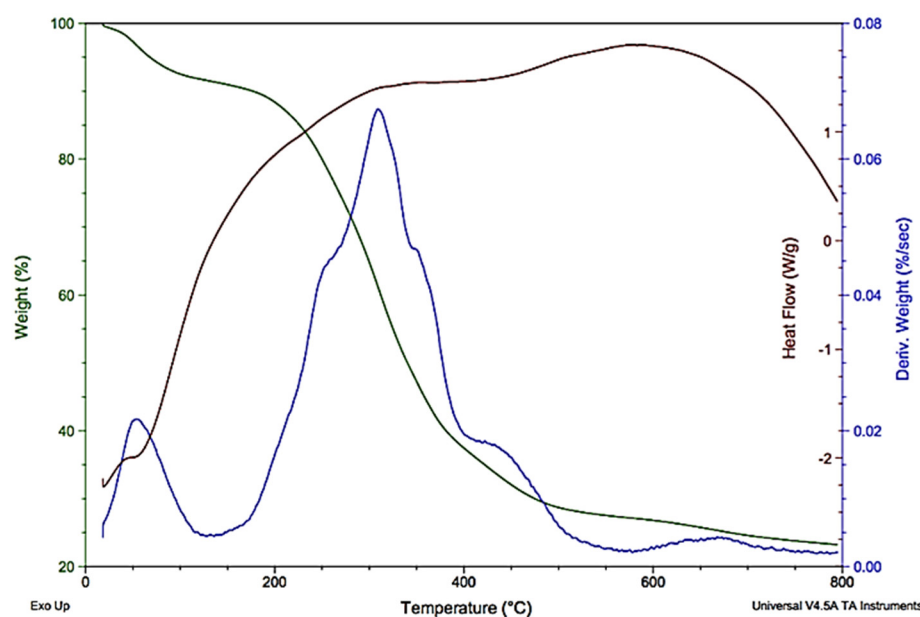

Figure 4. TGA/DTA Analysis.

3. Experimental Procedure

The adsorption tests were conducted, in triplicate, by adding 10 mg of activated carbon to 25 mL of the mixture, containing EBT dye. The stock concentration of the three mixtures was diluted to draw the calibration curve in a concentration range of EBT dye (from 10 to 70 mg.L^{-1}), and the absorbance measured using a spectrophotometer. The tests were disposed on a shaker with a stirring speed of 150 rpm. For adsorption kinetics, samples were taken at time intervals varying from 20 to 160 min, centrifuged for 2 min at 3000 rpm, and then the absorbance was measured. Regarding the isothermal tests, the initial concentrations used were 10; 20; 30; 40; 50; 60; and 70 mg.L^{-1}. Samples were taken after an equilibrium time of 90 min. The quantity of EBT adsorbed per gram of activated carbon q_e (mg.g^{-1}), was determined based on the following formula:

$$q_e = \frac{(C_i - C_e) \times V}{M} \tag{1}$$

$$R\% = \frac{(C_i - C_e)}{C_i} * 100 \tag{2}$$

where C_i and C_e are the initial and final ion concentrations, respectively, expressed in (mg.L^{-1}). V is the volume in liters of the solution and M represents the mass of activated carbon in (g), and R%: removal.

4. Results and Discussion

4.1. pH Effect

Figure 5 shows the effect of pH on the elimination of the dye, it is observed that with the increase in pH the quantity adsorbed reduces this decrease due to the presence of ions (H$^+$) which causes the birth of protonation of the OH groups to dye in the acid medium by elimination of the water molecule and formation of a cycle of seven with two nitrogen atoms. In the basic medium, the existence of ions (HO$^-$) in the solution inhibits the adsorption of the dye on the surface of the cannabis and the adsorption becomes very hard with a minimum quantity of 1.7 mg.g^{-1} at pH = 12.
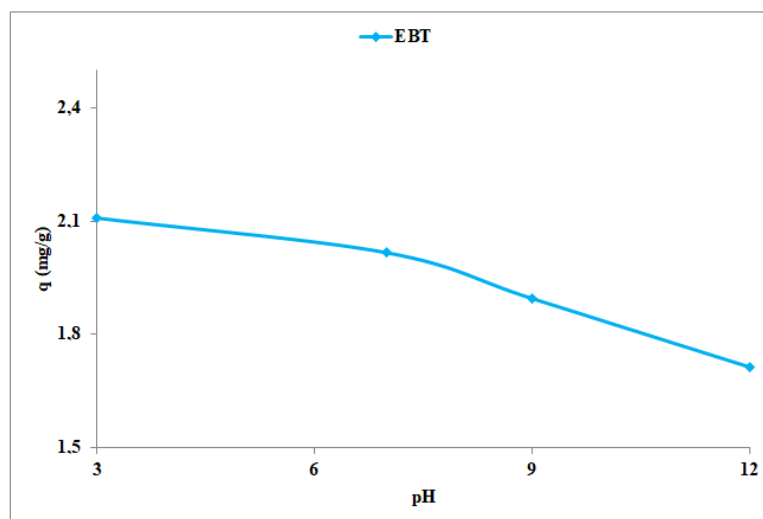
Figure 5. pH effect on the adsorption of EBT dye by activated carbon of cannabis (t = 90 min, T = 20 ± 1 °C, adsorbent dose 10 mg, (C_0 = 10 mg.L^{-1}), stirring speed = 150 rpm.

We present in (Equation (3)) the formula for predicting adsorption as a function of pH. This formula is obtained using polynomial interpolation. The interpolation error is given by the formula (Equation (4)).

$$Ad = 9.25926e - 5 \times pH^3 - 5.92593e - 3 \times pH^2 + 2.69444 \times pH + 2.07 \tag{3}$$

where, Ad is the value of the adsorption

$$\forall x \in [pH_{min}, pH_{max}] \, we \, have, \; Er = \frac{Ad^{(n+1)}(x)}{(n+1)!} \prod_{i=0}^{n} (x - pH_i) \tag{4}$$

where Er is the interpolation error, n is the polynomial degree. pH_{min} and pH_{max} are, respectively, the minimum and maximum pH values in the experiment. pH_i is the nth value of pH in the experiment. $Ad^{(n)}$ is the nth derivative of Ad, and $n! = n \times (n-1) \times \cdots \times 2 \times 1$. Figure 6 shows the comparison of the results of our model (Equation (3)) and the observed results.
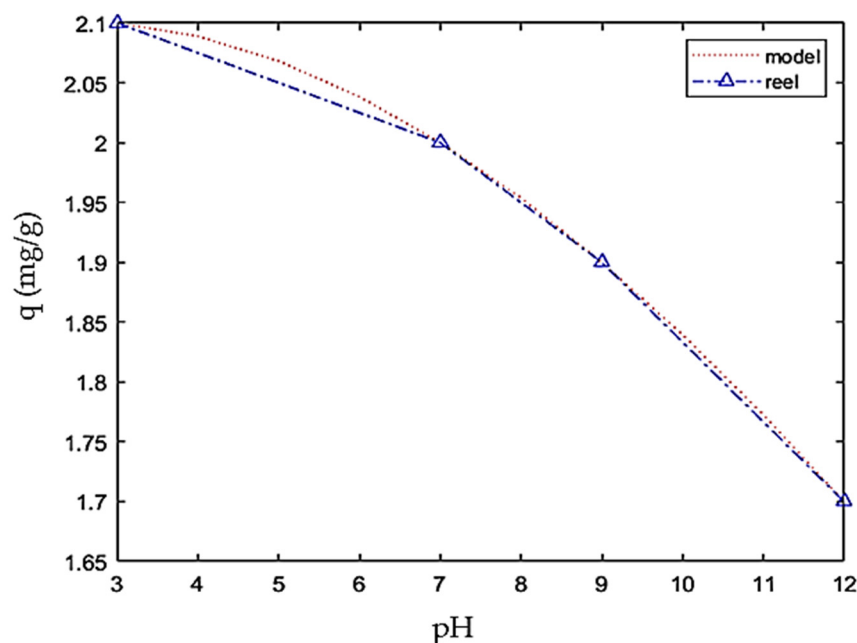
Figure 6. Comparison between the mathematical model (Equation (3)) and the observed results.

The coefficients in (Equation (3)) are calculated using the Lagrange interpolation formula given by:

$$Ad(pH) = \sum_{j=0}^{n} pH_i \left(\prod_{i=0, i \neq j}^{n} \frac{pH - pH_i}{pH_j - pH_i} \right)$$

4.2. Dose Effect

The histogram presented in Figure 7 gives the effect of the dose of cannabis on the elimination of the dye; it is observed that the yield increases with the increase in mass, this yield goes through 44.12% for m = 10 mg then continuously increases up to a yield of 60% when m = 40 mg, but for masses m $\geq$ 50 mg the yield remains almost constant, fixed at 62% at this moment in equilibrium.
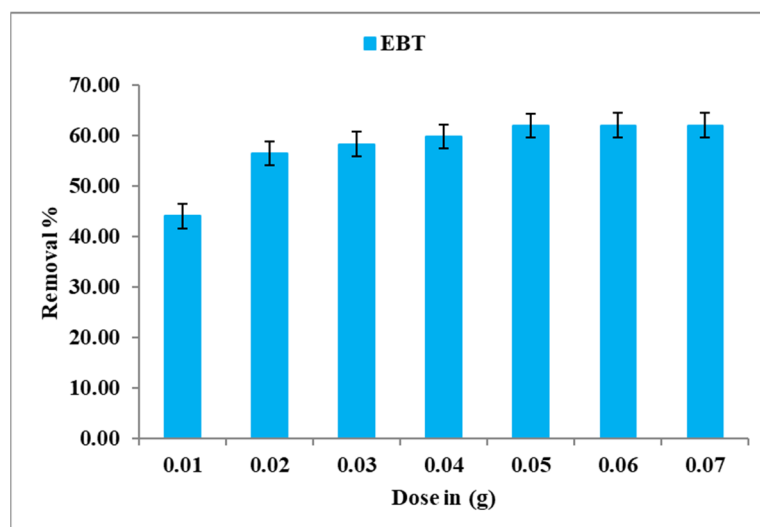

Figure 7. Influence of the mass of activated carbon of cannabis on adsorption of EBT dye (stirring speed = 150 rpm, *t* = 90 min, pH = 7 $\pm$ 0.2; C_0 = 10 mg.L^{-1} and temperature = 20 $\pm$ 1 °C).

The mathematical model describing the effect of the mass of the activated carbon on the adsorption of EBT is given by the formula (Equation (5)).

$$Re = 2.92222 \times 10^9 \times d^6 - 6.53083 \times 10^8 \times d^5 + 5.60264 \times 10^7 \times d^4$$
$$-2.31604 \times 10^6 \times d^3 + 47473.1 \times d^2 - 183.715 \times d + 0.673 \tag{5}$$

where Re is the removal and d is the dose in g. This formula is obtained by using the same technique used in (Equation (3)). We give in Figure 8 the comparison between our new mathematical model and the detected findings.
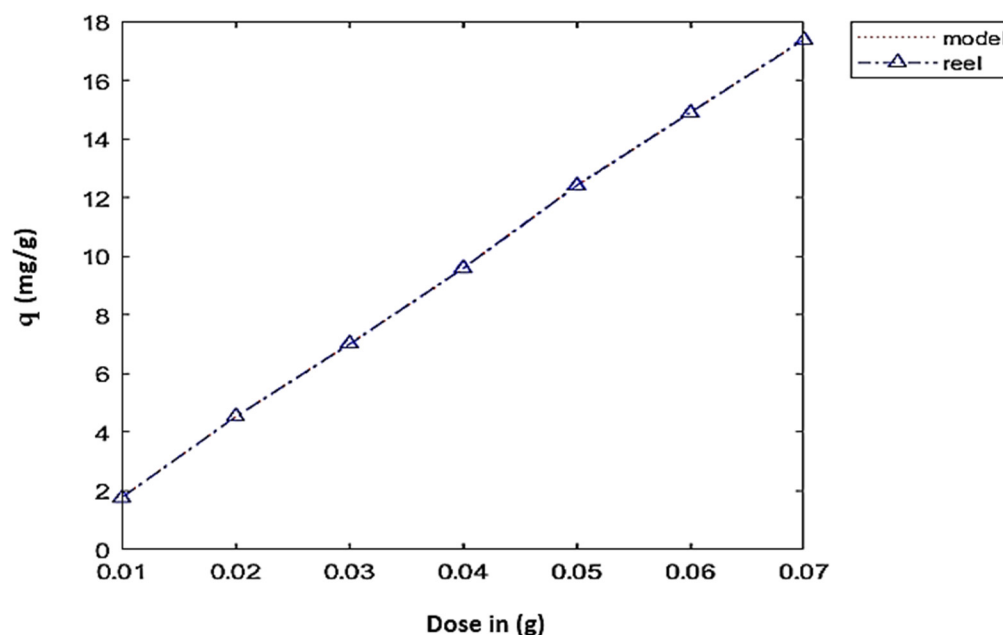
Figure 8. Comparison between the mathematical model and the observed results.

4.3. Effect of the Initial Concentration

With the aim to identify the impact of the preliminary concentration of EBT dye suggested for these studies on retention phenomena, solutions of 100 mL were prepared at different concentrations of metal ions between 10 to 70 mg.L^{-1}. The achieved results are presented in Figure 9 below. The illustrious results show that the adsorbed amount of EBT dye increases with increasing initial concentration. In fact, after an equilibrium time of 90 min, the adsorption capacity registers an increase from 2.21 to 10.17 mg.g^{-1}, for concentrations from 10 to 70 mg.L^{-1}. This action is explained by the fact that the more the concentration of EBT dye increases, the more the number of molecules in the solution increases, involving a higher absorption capacity [33–35].
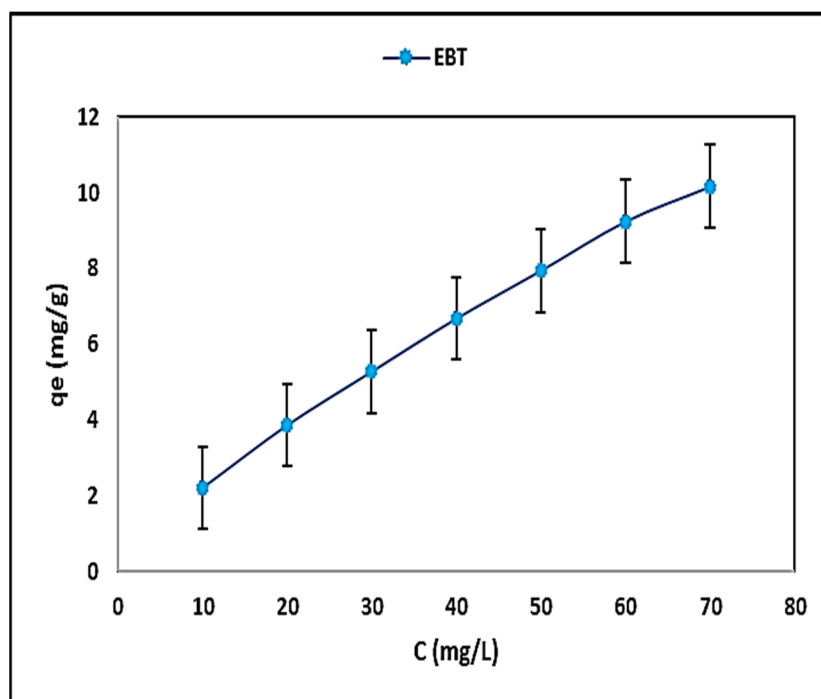
The mathematical model describing the effect of the initial concentration of EBT dye adsorption by activated carbon of cannabis is given by the formula (Equation (6)).

$$q_e = -\frac{11 \times c^6}{7.2e8} + \frac{91 \times c^5}{2.4e7} - \frac{107 \times c^4}{2.88e4} + \frac{291 \times c^3}{1.6e4} - \frac{1.6657 \times c^2}{3.6e4} + \frac{1753 \times c}{300} - 25 \tag{6}$$

where q_e is the amount adsorbed at equilibrium and c is the initial concentration of EBT in mg/L. This formula is obtained by using the same technique used in (Equation (3)).

The comparison between our new mathematical model and the observed results is given in Figure 10.

Figure 9. Effect of initial concentration of EBT dye adsorption by activated carbon of cannabis (t = 90 min, T = 20 $\pm$ 1 $^\circ$C, adsorbent dose 10 mg, stirring= 150 rpm and pH = 7 $\pm$ 0.2).
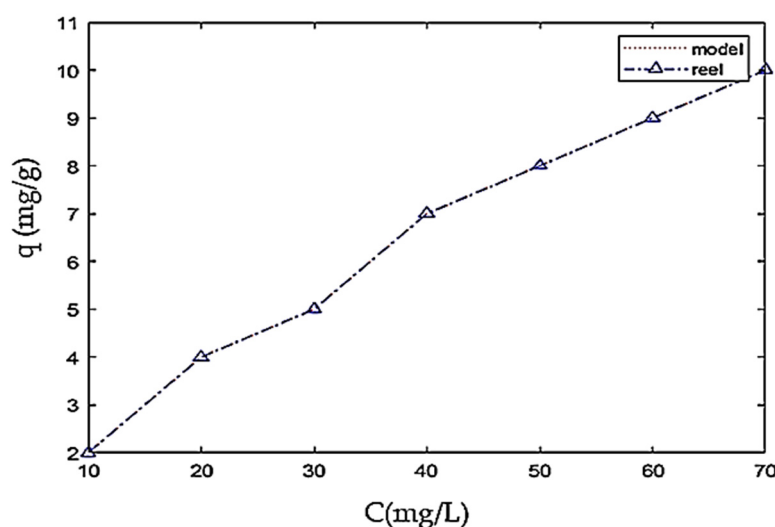

Figure 10. Comparison between the mathematical model and the observed results.

4.4. Effect of Contact Time

The adsorptions of Eriochrome Black T (EBT) by activated carbons obtained from hemp waste (*Cannabis sativa* L.) were studied at different time intervals (20 to 160 min) and a fixed amount of 10 mg.L^{-1}. Figure 11 shows that the absorption speed is fast during the first 20 to 60 min, and afterwards proceeds at a slower rate with a constant phenomenon of adsorption–desorption until the 100 min. After this period, the amount adsorbed did not change significantly. The initial rapid reaction is due to many vacant sites available at the initial stage; as a result, there is an increased concentration gradient between the adsorbate in the solution and the adsorbate in the adsorbent. Generally, the rapid initial adsorption results in a surface reaction. Slower adsorption ensues as available adsorption sites decrease with increasing occupancy and repulsive forces between favorable negatively

charged dye (EBT) adsorption due to electrostatic attraction molecules on the phase's solid and bulk [36]. The maximum absorption of EBT after reaching pseudo-equilibrium was 1.9 mg/g.
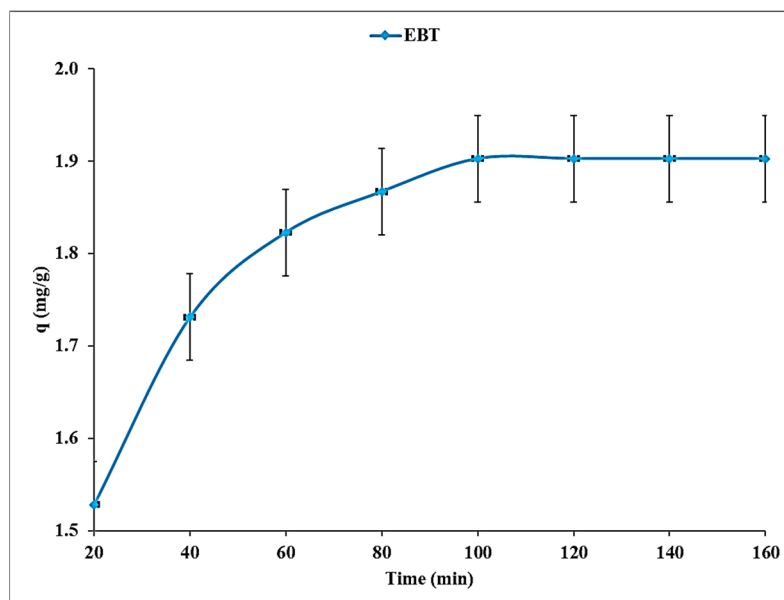
Figure 11. Effect of contact time of EBT dye adsorption by activated carbon of cannabis (T = 20 ± 1 °C, adsorbent dose 10 mg, C_0 = 10 mg.L^{-1}, stirring speed = 150 rpm and pH = 7 ± 0.2).

4.5. Effect of Temperature

The following figure represents the effect of temperature on the amount adsorbed by EBT on cannabis. From Figure 12, we observe that the temperature is a kinetic factor favoring the adsorption of the dye and also that the quantity adsorbed increases from 1.89 to 2 mg.g^{-1} when the temperature increases from 293°K to 313°K, then the continuous adsorbed amount increases up to 2.2 mg.g^{-1} when the temperature equals 333°K. This increase is owing to the effect of vibration of the dye molecules with the increase in shock numbers on the surface of the cannabis. Therefore, the adsorption of the examined ions seems to be an endothermic phenomenon. This could be also due to a relative increase in the mobility of ions in solution, which improves their exposure to active adsorption sites on the one hand and sends them to difficult-to-access sites on the other.
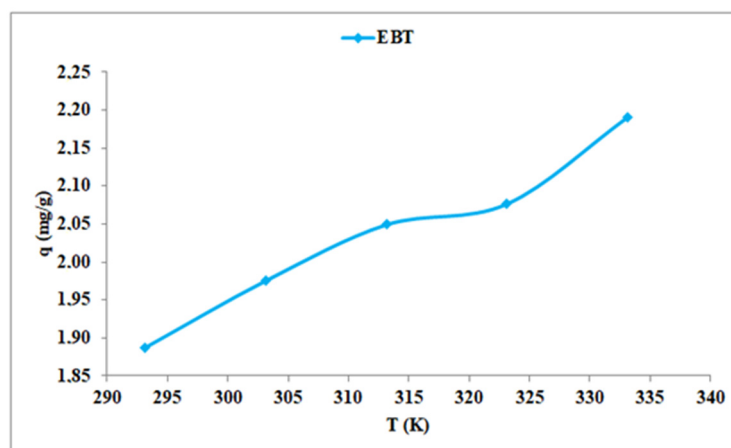
Figure 12. Effect of temperature of EBT dye adsorption by activated carbon of cannabis (adsorbent dose 10 mg, C_0 = 10 mg.L^{-1}, stirring speed = 150 rpm and pH = 7 ± 0.2).

4.6. Modeling of Adsorption Isotherms

To obtain the adsorption isotherm, a series of Erlenmeyer flasks were employed. In each Erlenmeyer were poured 25 mL of EBT solution dye of varying concentrations: 10; 20; 30; 40; 50; 60 and 70 mg.L^{-1}. The adsorption equilibrium study was carried out under the same optimum conditions mentioned above. After equilibration, the particles of the adsorbent were separated by centrifugation and the clarified mixture was analyzed by determination of the equilibrium concentration (C_e) of EBT using the same calibration curve used previously. The quantity of the adsorbed reagent at equilibrium (q_e, in mg.g^{-1}) was calculated by an equation (Equation (1)).

The following four conventional models, in their linear forms, are used to describe the adsorption isotherms:

The four models tested in this adsorption are presented by their nonlinear equation and also their linear form.

The Langmuir model (Equation (7)) is linearized according to the form given in (Equations (8) and (9)) [37,38] the linear form of the Freundlich model (Equation (9)) [39,40], the Temkin model (Equation (10)) [41], and finally the Dubinin–Radushkevich model (Equation (11)) [42], the potential of Polanyi (Equation (12)) energy (Equation (13)) [43]

$$q_e = \frac{q_m \, K_L C_e}{1 + K_L C_e} \tag{7}$$

$$\left(\frac{1}{q_e} \right) = \frac{1}{q_m K_L} \left(\frac{1}{C_e} \right) + \frac{1}{q_m} \tag{8}$$

$$R_L = \frac{1}{1 + K_L C_0} \tag{9}$$

$$Ln \, q_e = \frac{1}{n} \, Ln \, C_e + Ln \, K_F \tag{10}$$

$$q_e = \frac{RT}{b} \, Ln \, C_e + \frac{RT}{b} Ln \, K_T \tag{11}$$

$$Ln \, q_e = -K_D \, \varepsilon^2 + Ln \, q_m \tag{12}$$

$$\varepsilon = RTLn \left(1 + \frac{1}{C_e} \right) \tag{13}$$

$$E = \frac{1}{\sqrt{2K_D}} \tag{14}$$

Figure 13 represents the representation of the four linear forms of these isotherms and the choice of the model is subject to the correlation factor of the experimental points.

The linearization and the graphic representation of the four models tested in this study, and the obtained results synthesized in Table 2 above, indicate that the value of the linear correlation coefficient for the Freundlich model is closer to 1 for the EBT dye studied; these results also show the high value of the maximum adsorption capacity for the Langmuir model was 14.03 mg.g^{-1}. Similarly, some studies were written on the absorption phenomena of other such ions and dyes [44–52] (Table 3).

4.7. Modeling of Adsorption Kinetics

To evaluate the reaction parameters, a modeling of the adsorption kinetics is essential for the identification of the chemical or physical mechanisms that control the rate of adsorption. Four models are employed to link the experimental data of the absorption kinetics of the studied systems, namely pseudo-first order, pseudo-second order, and intraparticle diffusion models. Figure 14 and Table 4 show the adsorption Kinetics obtained in this study.
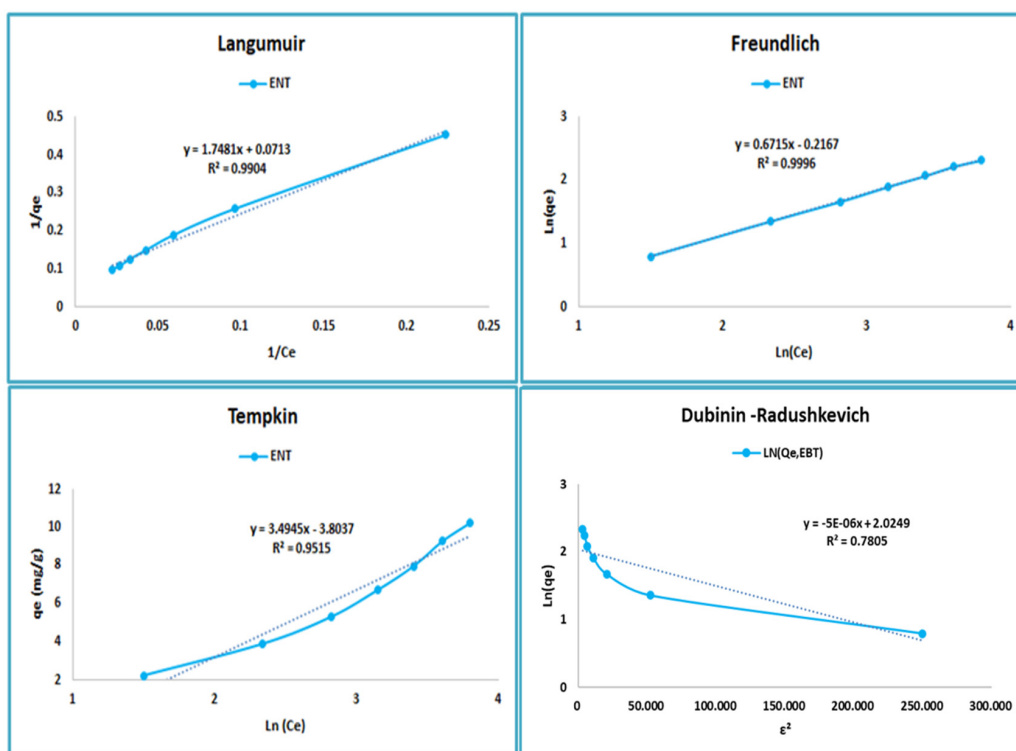
Table 2. Constant adsorption of four isotherms models of EBT dye on activated carbon of cannabis (T = 20 ± 1 °C, mass of adsorbent = 10 mg, stirring speed = 150 rpm and pH = 7 ± 0.2).

| Isotherm Models	Constants	Activated Carbon of Cannabis
Langmuir	**R^2**	**0.9904**
	R_L	0.2636–0.7143
	K_L (L.mg^{-1})	0.0399
	q_m (mg.g^{-1})	14.025
Freundlich	**R^2**	**0.9996**
	K_F	0.8052
	n	1.4892
Temkin	**R^2**	**0.9545**
	K_T (L.g^{-1})	0.00012
	B_1 (J.mol^{-1})	3.4945
	b	697.096
Dubinin–Radushkevich	R^2	0.7805
	K_{ad} (mol^2.Kj^{-2}) $\times 10^{-5}$	0.5
	E (Kj.mol^{-1})	316.2277
	q_m (mg.g^{-1})	7.5754

Table 3. The adsorption capacity of dyes and heavy metals in aqueous solutions by activated carbons of different biomass.

Adsorbate	Adsorbent Pollutants	Dose (mg)	C_0 (mg L^{-1})	pH	Kinetic	Isotherm	q_m (mg g^{-1})	Ref.
Zinc oxide-loaded activated char (ZnO-AC)	OG Rh-b	8–30	50	7	Pseudo-second-order	Lang-muir	153.8 128.2	[46]
Rice straw (RS) biochar Wood chip (WC) biochar	CV-CR	01	500	7	Pseudo-second-order	Langmuir	620.3 195.6	[47]
Charcoal (tree branches) (BCA-TiO₂)	MB Cd^{2+}	** **	0.4 600	7 8	Pseudo-second-order	**	200 250	[48]
Sulfonated peanut shell (PNS-SO3H)	MB TC	20	900 ppm	10	Pseudo-second-order	Langmuir	1250 303	[49,50]
Shrimp shell (SS) Coal acid mine drainage (AMD)	Mn Fe	**	≤1 ≤15	6–9 5–9	Pseudo-second-order	Frendlich	17.43 3.87	[51]
Waste hemp activated carbon (WHAC)	EBT	10	10	7	Pseudo-second-order	Langmuir	14.025	This work

** Undetermined.

Figure 13. Langmuir, Freundlich, Temkin, and Dubinin–Radushkevich isotherm models curves of activated carbon of cannabis adsorption towards BET dye.
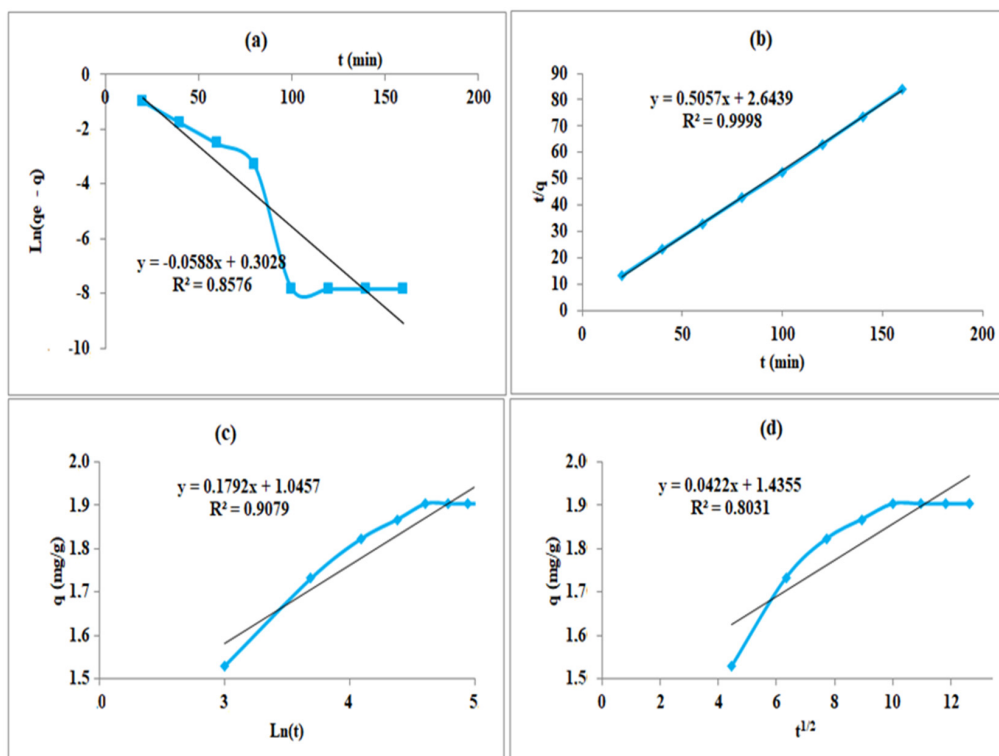
Figure 14. Adsorption kinetics models: (**a**) pseudo-first-order, (**b**) pseudo-second-order, (**c**) Elovich and (**d**) interparticle diffusion of BET dye on activated carbon of cannabis, (T = 20 $\pm$ 1 °C, adsorbent dose 10 mg, C_o = 10 mg.L^{-1}, stirring = 150 rpm and pH = 7 $\pm$ 0.2).

Table 4. Adsorption kinetics constants of BET dye on activated carbon cannabis (temperature = 20 ± 1 °C, mass of adsorbent = 10 mg, initial concentration of dye = 10 mg.L^{-1}; stirring speed = 150 rpm and pH = 7 ± 0.2).

Models	The Constants	Cannabis
Pseudo-first-order	R^2	0.8576
	K_1 (mL.min^{-1})	0.0588
	$q_{e,cal}$ (mg.g^{-1})	1.353
	$q_{e,exp}$ (mg.g^{-1})	1.903
Pseudo-second-order	R^2	0.9998
	K_2 (g.mg^{-1}.min^{-1})	0.0968
	$q_{e,cal}$ (mg.g^{-1})	1.9774
	$q_{e,exp}$ (mg.g^{-1})	1.903
Elovich	R^2	0.9079
	α (mg.g^{-1}.min^{-1})	45.4475
	β (g.mg^{-1})	5.5803
Intraparticle diffusion	R^2	0.8031
	K_i (mg.g^{-1}.min$^{0.5}$)	0.0422
	C (mg.g^{-1})	1.4355

For a pseudo-first-order kinetics, Lagergen suggested in 1898 [53] the following equation:

$$\frac{dq}{dt} = K_1(q_e - q) \tag{15}$$

From the integration of (Equation (13)) and the application of the boundary conditions we find the following equation:

$$Ln(q_e - q_t) = Ln(q_e) - K_1 t \tag{16}$$

The pseudo-second-order model, or the Ho and Mckay model [54,55], turns out to be more appropriate for writing experimental data; this model is given by its following linear equation:

$$\frac{t}{q_t} = \frac{1}{K_2 q_e^2} + \left(\frac{1}{q_e}\right)t \tag{17}$$

The models established, respectively, by Morris and Weber and Urano Tachikawa [56] for internal diffusion were used with the aim of selecting the model or models best suited to the physical processes implicated in the adsorption of adsorbate on the activated carbon of cannabis used. This model is expressed in the following form:

$$q_t = K_i t^{\frac{1}{2}} + C \tag{18}$$

With: t the time in (min); q_e: the amount adsorbed at equilibrium (mg.g^{-1}); q_t: the quantity adsorbed at the instant t (mg.g^{-1}); K_1: the first-order rate constant (min^{-1}); K_2: the second-order rate constant (g.mg^{-1}.min^{-1}); C: the boundary layer thickness value (mg.g^{-1}); K_i: diffusion speed coefficient (min$^{-1/2}$).

4.8. Thermodynamic Study

The thermodynamic parameters were determined to qualify the phenomenon of absorption of EBT dye on activated carbon of cannabis. Thus, Gibbs free energy or free enthalpy of absorption; $\Delta G°$ (kJ.mol^{-1}), the enthalpy of adsorption; $\Delta H°$ (kJ.mol^{-1})

and adsorption entropy; ΔS° (KJ.mol^{-1}.K^{-1}) were calculated according to equations (Equations (18) and (19)) [52].

$$\Delta G^0 = -RT.Ln(K_d) \tag{19}$$

$$Ln(K_d) = -\frac{\Delta H^0}{RT} + \frac{\Delta S^0}{R} \tag{20}$$

$$K_d = \frac{q_e}{C_e} \tag{21}$$

where, K_d is the adsorption equilibrium constant, R is the gas constant perfect, and T is the temperature in (°K). From the results illustrated in Table 5 and Figure 15, the positive value of (ΔS°) shows the good nature of the present adsorption phenomenon. Furthermore, positive values of (ΔG°) show that the examined adsorption process is spontaneous up to a temperature of 60 °C. In addition, the positive value of (ΔH°) demonstrates the endothermic nature of this phenomenon.

Table 5. Thermodynamics parameters data of EBT dye adsorption on activated carbon of cannabis.

Parameters		Cannabis
ΔH° (KJ.mol^{-1})		16.8467
ΔS° (J.mol^{-1}.K^{-1})		11.0808
ΔG° (kJ.mol^{-1})	T = 293°K	13.5999
	T = 303°K	13.48917
	T = 313°K	13.37838
	T = 323°K	13.26756
	T = 333°K	13.15675
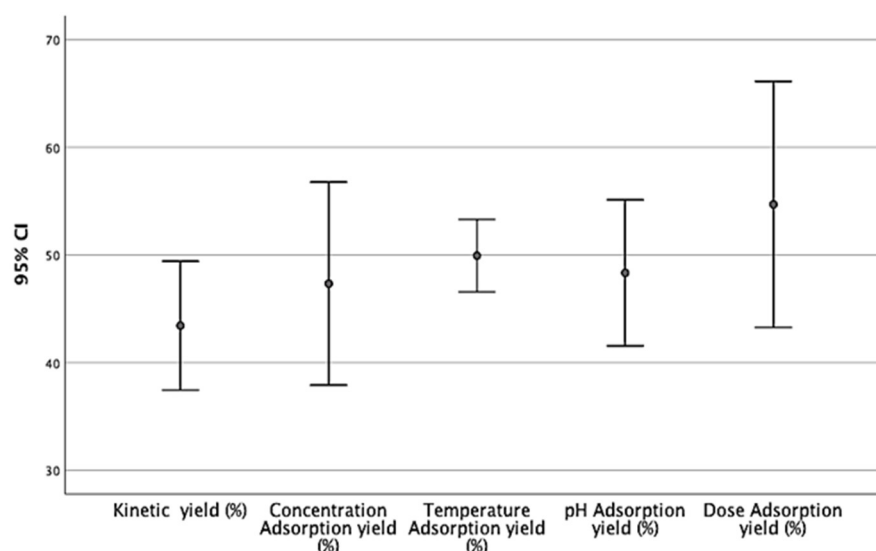
Figure 15. The 95% confidence intervals for the main analysis of influential adsorption parameters.

5. Conclusions

In this study, the performance of phosphoric acid-activated carbonaceous materials derived from waste hemp (*Cannabis sativa* L.) to remove Eriochrome Black T (EBT) from an aqueous mixture was investigated. The effects of the activator (liquid) to adsorbent (solid) on the textural, structural, and adsorption characteristics were investigated. The porosity of the adsorbents increased with increasing the activator: adsorbent ratios resulting in increased adsorption capacities. Equilibrium data were well explained by the Langmuir model with upper limit adsorption abilities of 14.03 mg.g^{-1} for WHAC corresponding to

the activator: adsorbent ratios of 1:1. The second-order kinetic model was suitable with the experimental results. It was found that the prepared activated carbons worked as a potent adsorbent for the elimination of EBT from an aqueous medium. Since the *Cannabis sativa* L. plant is available in abundance in Morocco, it may be considered as an economically viable raw material.

References

1. Farinon, B.; Molinari, R.; Costantini, L.; Merendino, N. The seed of industrial hemp (*Cannabis sativa* L.): Nutritional quality and potential functionality for human health and nutrition. *Nutrients* **2020**, *12*, 1935. [CrossRef] [PubMed]
2. Russo, E.B.; Jiang, H.E.; Li, X.; Sutton, A.; Carboni, A.; del Bianco, F.; Mandolino, G.; Potter, D.J.; Zhao, Y.X.; Bera, S.; et al. Phytochemical and genetic analyses of ancient cannabis from Central Asia. *J. Exp. Bot.* **2008**, *59*, 4171–4182. [CrossRef] [PubMed]
3. Andre, C.M.; Hausman, J.-F.; Guerriero, G. Cannabis sativa: The plant of the thousand and one molecules. *Front. Plant Sci.* **2016**, *7*, 19. [CrossRef] [PubMed]
4. De Petrocellis, L.; Ligresti, A.; Moriello, A.S.; Allarà, M.; Bisogno, T.; Petrosino, S.; Stott, C.G.; Di Marzo, V. Effects of cannabinoids and cannabinoid-enriched Cannabis extracts on TRP channels and endocannabinoid metabolic enzymes. *Br. J. Pharmacol.* **2011**, *163*, 1479–1494. [CrossRef]
5. Zhang, J.; Mao, L.; Nithya, K.; Loh, K.C.; Dai, Y.; He, Y.; Tong, Y.W. Optimizing mixing strategy to improve the performance of an anaerobic digestion waste-to-energy system for energy recovery from food waste. *Appl. Energy* **2019**, *249*, 28–36. [CrossRef]
6. Wang, B.; Dong, F.; Chen, M.; Zhu, J.; Tan, J.; Fu, X.; Wang, Y.; Chen, S. Advances in recycling and utilization of agricultural wastes in China: Based on environmental risk, crucial pathways, influencing factors, Policy Mechanism. *Procedia Environ. Sci.* **2016**, *31*, 12–17. [CrossRef]
7. Sulyman, M.; Namiesnik, J.; Gierak, A. Low-cost Adsorbents Derived from Agricultural By-products/Wastes for Enhancing Contaminant Uptakes from wastewater: A Review. *Polish J. Environ. Stud.* **2017**, *26*, 479–510. [CrossRef]
8. Crini, G.; Badot, P.M. *Traitement et Epuration des Eaux Industrielles Polluées*; Presses Universitaires de Franche-Comté: Besançon, France, 2007; p. 353.
9. Sidi Zhu, Mingzhu Xia, Yuting Chu, Muhammad Asim Khan, Wu Lei, Fengyun Wang, Tahir Muhmood, Along Wang, Adsorption and Desorption of Pb(II) on l-Lysine Modified Montmorillonite and the simulation of Interlayer Structure. *Appl. Clay Sci.* **2019**, *169*, 40–47. [CrossRef]
10. Zhu, Sidi and Chen, Yexiang and Khan, Muhammad Asim and Xu, Haihua and Wang, Fengyun and Xia, Mingzhu, In-Depth Study of Heavy Metal Removal by an Etidronic Acid-Functionalized Layered Double Hydroxide. *ACS Appl. Mater. Interfaces* **2022**, *14*, 7450–7463. [CrossRef]
11. Chen, Y.; Zhu, Y.; Wang, Z.; Li, Y.; Wang, L.; Ding, L. Application of studies of activated carbon derived from rice husks produced by chemical–thermal process—A review. *Adv. Colloid Interface Sci.* **2011**, *163*, 39–52. [CrossRef]
12. Iqbal, M.J.; Ashiq, M.N. Adsorption of dyes from aqueous solutions on activated charcoal. *J. Hazard Mater.* **2007**, *139*, 57–66. [CrossRef] [PubMed]
13. Monvisade, P.; Siriphanon, P. Chitosan intercalated montmorillonite: Preparation, characterization and cationic dye adsorption. *Appl. Clay Sci.* **2009**, *42*, 427–431. [CrossRef]
14. Tan, I.A.; Ahmad, A.L.; Hameed, B.H. Adsorption of basic dye using activated carbon prepared from oil palm shell: Batch and fixed bed studies. *Desalin* **2008**, *225*, 13–28. [CrossRef]
15. Amin, N.K. Removal of direct blue-106 dye from aqueous solution using new activated carbons developed from pomegranate peel: Adsorption equilibrium and kinetics. *J. Hazard Mater.* **2009**, *165*, 52–62. [CrossRef]

16. da Silva, L.G.; Ruggiero, R.; Gontijo, P.M.; Pinto, R.B.; Royer, B.; Lima, E.C.; Fernandes, T.H.M.; Calvete, T.A. Adsorption of Brilliant Red 2BE dye from water solutions by a chemically modified sugarcane bagasse lignin. *Chem. Eng. J.* **2011**, *168*, 620–628. [CrossRef]

17. Mansouri, F.E.; Farissi, H.E.; Zerrouk, M.H.; Cacciola, F.; Bakkali, C.; Brigui, J.; Lovillo, M.P.; Esteves da Silva, J.C.G. Dye Removal from Colored Textile Wastewater Using Seeds and Biochar of Barley (*Hordeum vulgare* L.). *Appl. Sci.* **2021**, *11*, 5125. [CrossRef]

18. Rajeshwarisivaraj, C.; Namasivayam, K.; Kadirvelu, K. Orange peel as an adsorbent in the removal of Acid violet 17 (acid dye) from aqueous solutions. *Waste Manag.* **2001**, *21*, 105–110.

19. Sudaryanto, Y.; Hartono, S.; Irawata, W.; Hidarso, H.; Ismadji, S. High surface area activated carbons prepared from cassava peel by chemical activation. *Bioresour Technol.* **2006**, *97*, 734–739. [CrossRef]

20. Patnukao, P.; Pavasant, P. Activated carbon from eucalyptus camaldulensis dehn barkusing phosphoric acid activation. *Bioresour. Technol.* **2008**, *99*, 8540–8543. [CrossRef]

21. Gratuito, M.; Panyathanmaporn, T.; Chumnanklong, R.; Sirinuntawittaya, N.; Dutta, A. Production of activated carbon from coconut shell: Optimization using response surface methodology. *Bioresour Technol* **2008**, *99*, 4887–4895. [CrossRef]

22. Ozer, C.; Imamoglu, M.; Turhan, Y.; Boyan, F. Removal of methylene blue from aqueous solutions using phosphoric acid activated carbon produced from hazelnut husks. *Toxic Environ. Chem.* **2012**, *94*, 1283–1293. [CrossRef]

23. Li, W.; Zhang, L.; Peng, J.; Li, N.; Zhu, X. Preparation of high surface activated carbons from tobacco stems with K2CO3 activation using microwave irradiation. *Ind. Crop. Prod.* **2008**, *27*, 341–347. [CrossRef]

24. Rim, B.A.; Sarra, K.; Karine, M.; Achraf, G. Adsorptive removal of cationic and anionic dyes from aqueous solution by utilizing almond shell as bioadsorbent. *Euro-Mediterr. J. Environ. Integr.* **2017**, *2*, 20. [CrossRef]

25. Ghader, Z.; Mahsa, K.; Yusef, O.K.; Heshmatollah, N.; Shirin, E.; Mohammad, J.M.; Rajab, R. Eriochrme black-T removal from aqueous environment by surfactant modified clay: Equilibrium, kinetic, isotherm, and thermodynamic studies. *Toxin Rev.* **2018**, *38*, 307–317. [CrossRef]

26. el Farissi, H.; Lakhmiri, R.; Albourine, A.; Safi, M.; Cherkaoui, O. Adsorption study of charcoal of cistus ladaniferus shell modified by H3PO4 and NaOH used as a low-cost adsorbent for the removal of toxic reactive red 23 dye: Kinetics and thermodynamics. *Mater. Today Proc.* **2020**, *43*, 1740–1748. [CrossRef]

27. El Mansouri, F.; El Farissi, H.; Cacciola, F.; Talhaoui, A.; El Bachiri, A.; Tahani, A.; Esteves da Silva, J.C.G.; Brigui, J. Rapid elimination of copper (II), nickel (II) and chromium (VI) ions from aqueous solutions by charcoal modified with phosphoric acid used as a green biosorbent. *Polym. Adv. Technol.* **2022**, *33*, 2254–2264. [CrossRef]

28. Molina-Sabio, M.; Rodríguez-Reinoso, F. Role of chemical activation in the development of carbon porosity. *Colloids Surf. A Physicochem. Eng. Asp.* **2004**, *241*, 15–25. [CrossRef]

29. Foong, S.Y.; Liew, R.K.; Yang, Y.; Cheng, Y.W.; Yek, P.N.Y.; Mahari, W.A.W.; Lee, X.Y.; Han, C.S.; Vo, N.D.-V.; Le, Q.V.; et al. Valorization of biomass waste to engineered activated biochar by microwave pyrolysis: Progress, challenges, and future directions. *Chem. Eng. J.* **2020**, *389*, 124401. [CrossRef]

30. Zięzio, M.; Charmas, B.; Jedynak, K.; Hawryluk, M.; Kucio, K. Preparation and characterization of activated carbons obtained from the waste materials impregnated with phosphoric acid(V). *Appl. Nanosci.* **2020**, *10*, 4703–4716. [CrossRef]

31. Haykiri-Acma, H.; Yaman, S.; Alkan, M.; Kucukbayrak, S. Mineralogical characterization of chemically isolated ingredients from biomass. *Energy Convers. Manag.* **2014**, *77*, 221–226. [CrossRef]

32. Protásio, T.D.P.; Guimarães, M.; Mirmehdi, S.; Trugilho, P.F.; Napoli, A.; Knovack, K.M. Combustion of biomass and charcoal made from babassu nutshell. *Cerne* **2017**, *23*, 1–10. [CrossRef]

33. Park, D.; Yun, Y.S.; Park, J.M. Use of dead fungal biomass for the detoxification of hexavalent chromium: Screening and kinetics. *Process Biochem.* **2005**, *40*, 2559–2565. [CrossRef]

34. Begum, S.A.S.; Tharakeswar, Y.; Kalyan, Y.; Naidu, G.R. Biosorption of Cd (II), Cr (VI) Pb (II) from Aqueous Solution Using *Mirabilis jalapa* as Adsorbent. *J. Encapsulation Adsorpt. Sci.* **2015**, *5*, 93–104. [CrossRef]

35. Kondapalli, S.; Mohanty, K. Influence of Temperature on Equilibrium, Kinetic and Thermodynamic Parameters of Biosorption of Cr(VI) onto Fish Scales as Suitable Biosorbent. *J. Water Resour. Prot.* **2011**, *3*, 429–439. [CrossRef]

36. Dula, T.; Siraj, K.; Kitte, S.A. Adsorption of Hexavalent Chromium from Aqueous Solution Using Chemically Activated Carbon Prepared from Locally Available Waste of Bamboo (*Oxytenanthera abyssinica*). *ISRN Environ. Chem.* **2014**, *2014*, 4382452014. [CrossRef]

37. Langmuir, I. The Adsorption Of Gases On Plane Surfaces Of Glass, Mica And Platinum. *Verh. Deut. Phys. Ges.* **1918**, *40*, 1361–1403. [CrossRef]

38. Freundlich, H. *Colloid and Capilary Chemistry*, english translation of 3rd German ed.; Methuen: London, UK, 1926.

39. Freundlich, H.; Heller, W. The Adsorption of cis- and trans-Azobenzene. *J. Am. Chem. Soc.* **2002**, *61*, 2228–2230. [CrossRef]

40. Mahmoodi, N.M.; Salehi, R.; Arami, M.; Bahrami, H. Dye removal from colored textile wastewater using chitosan in binary systems. *Desalination* **2011**, *267*, 64–72. [CrossRef]

41. Ghasemi, M.; Javadian, H.; Ghasemi, N.; Agarwal, S.; Gupta, V.K. Microporous nanocrystalline NaA zeolite prepared by microwave assisted hydrothermal method and determination of kinetic, isotherm and thermodynamic parameters of the batch sorption of Ni (II). *J. Mol. Liq.* **2016**, *215*, 161–169. [CrossRef]

42. Wang, X.; Jiang, C.; Hou, B.; Wang, Y.; Hao, C.; Wu, J. Carbon composite lignin-based adsorbents for the adsorption of dyes. *Chemosphere* **2018**, *206*, 587–596. [CrossRef] [PubMed]

43. Shi, T.; Xie, Z.; Zhu, Z.; Shi, W.; Liu, Y.; Liu, M. Highly efficient and selective adsorption of heavy metal ions by hydrazide-modified sodium alginate. *Carbohydr. Polym.* **2022**, *276*, 118797. [CrossRef] [PubMed]

44. Maneechakr, P.; Mongkollertlop, S. Investigation on adsorption behaviors of heavy metal ions (Cd^{2+}, Cr^{3+}, Hg^{2+} and Pb^{2+}) through low-cost/active manganese dioxide-modified magnetic biochar derived from palm kernel cake residue. *J. Environ. Chem. Eng.* **2020**, *8*, 104467. [CrossRef]

45. Tao, Y.; Yang, B.; Wang, F.; Yan, Y.; Hong, X.; Xu, H.; Xia, M.; Wang, F. Green synthesis of MOF-808 with modulation of particle sizes and defects for efficient phosphate sequestration. *Sep. Purif. Technol.* **2022**, *300*, 121825. [CrossRef]

46. Saini, J.; Garg, V.K.; Gupta, R.K.; Kataria, N. Removal of Orange G and Rhodamine B dyes from aqueous system using hydrothermally synthesized zinc oxide loaded activated carbon (ZnO-AC). *J. Environ. Chem. Eng.* **2017**, *5*, 884–892. [CrossRef]

47. Sewu, D.D.; Boakye, P.; Woo, S.H. Highly efficient adsorption of cationic dye by biochar produced with Korean cabbage waste. *Bioresour. Technol.* **2017**, *224*, 206–213. [CrossRef]

48. Popa, N.; Visa, M. The synthesis, activation and characterization of charcoal powder for the removal of methylene blue and cadmium from wastewater. *Adv. Powder Technol.* **2017**, *28*, 1866–1876. [CrossRef]

49. Islam, M.T.; Hyder, A.G.; Saenz-Arana, R.; Hernandez, C.; Guinto, T.; Ahsan, M.A.; Alvarado-Tenorio, B.; Noveron, J.C. Removal of methylene blue and tetracycline from water using peanut shell derived adsorbent prepared by sulfuric acid reflux. *J. Environ.Chem. Eng.* **2019**, *7*, 102816. [CrossRef]

50. Isa, K.M.; Daud, S.; Hamidin, N.; Ismail, K.; Saad, S.A.; Kasim, F.H. Thermogravimetric analysis and the optimisation of bio-oil yield from fixed-bed pyrolysis of rice husk using response surface methodology (RSM). *Ind. Crops Prod.* **2011**, *33*, 481–487. [CrossRef]

51. Núñez-gómez, D.; Rodrigues, C.; Rubens, F. Adsorption of heavy metals from coal acid mine drainage by shrimp shell waste: Isotherm and continuous-flow studies. *J. Environ. Chem. Eng.* **2019**, *7*, 102787. [CrossRef]

52. Ho, Y.S.; McKay, G. Pseudo-second order model for sorption processes. *Process Biochem.* **1999**, *34*, 451–465. [CrossRef]

53. Urano, K.; Hirotaka, T. Process development for removal and recovery of phosphorus from wastewater by a new adsorbent. II. Adsorption rates and breakthrough curves. *Ind. Eng. Chem. Res.* **1991**, *30*, 1897–1899. [CrossRef]

54. Venkat, P.V.V.B.; Mane, S. Studies on the adsorption of Brilliant Green dye from aqueous solution onto low-cost NaOH treated saw dust. *Desalination* **2011**, *273*, 321–329. [CrossRef]

55. Jin, G.P.; Wang, X.L.; Fu, Y.; Do, Y. Preparation of tetraoxalyl ethylenediamine melamine resin grafted-carbon fibers for nano-nickel recovery from spent electroless nickel plating baths. *Chem. Eng. J.* **2012**, *203*, 440–446. [CrossRef]

56. Mahjoub, B.; Ncibi, M.C.; Seffen, M. Adsorption d'un Colorant Textile Réactif sur un Biosorbant Non-Conventionnel: Les Fibres de *Posidonia oceanica* (L.) Delile. *Can. J. Chem. Eng.* **2008**, *86*, 23–29. [CrossRef]